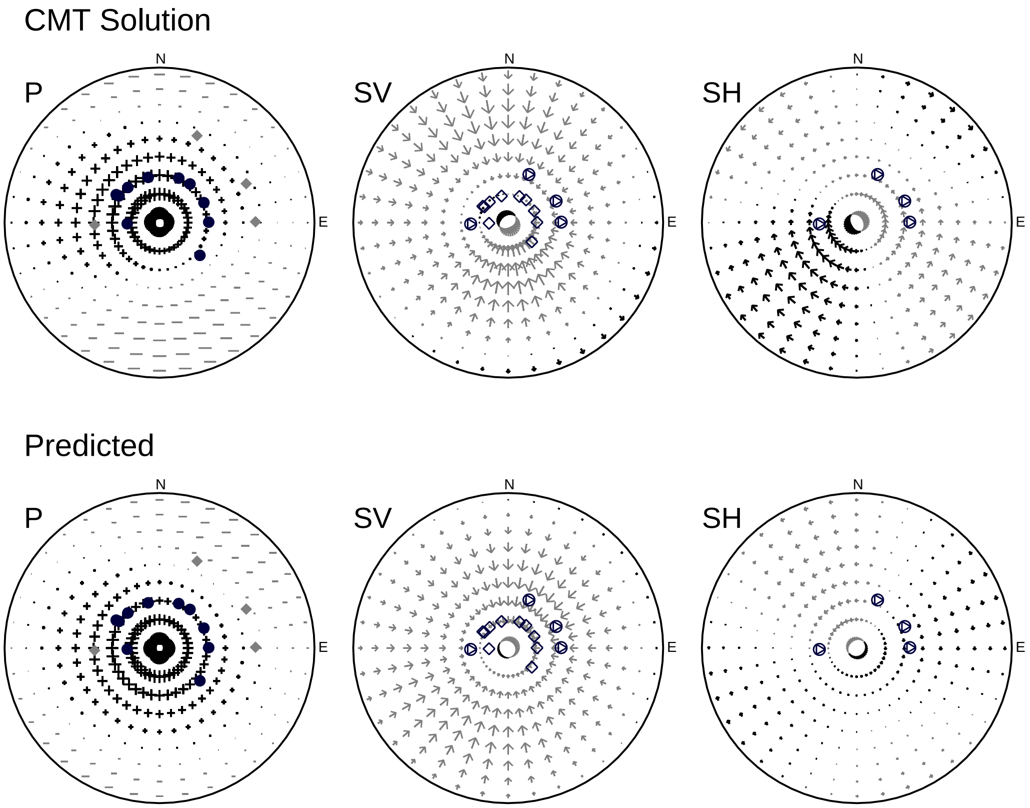

Fig. 5.19. Source radiation patterns for *P*, *SV* and *SH* waves for the Kyrgyzstan event, using the CMT solution (top), and the predicted source mechanism obtained from the inversion (bottom). The plotted symbols represent the average take-off angle and azimuth for various phases; solid circles for *P*, solid triangles for *pP*, solid (grey) diamonds for *pS*; open circles for *S*, open triangles for *sS*, and open diamonds for *sP*.

since only *P* energy is generated at the source for nuclear explosions, however we might observe *SV* wave energy due to *P*-to-*S* conversions between the source and receiver. No detectable *S* wave energy is observed at any of the stations for this event, and this information can be used as a constraint in the inversion. We attempted to perform a joint *P* and *S* inversion, however, since we are using a relative amplitude approach the inversion tries to match the noise, producing predicted seismograms with a false *S* signal. One way to overcome this might be to input zero amplitude 'observed' *S* wave traces, and perform a joint *P* and *S* inversion, however this approach did not work either. Therefore the following discussion is based on inversion with just the *P* waveforms. The waveforms are bandpass filtered in the range 0.01 Hz to 1.5 Hz before inversion.

A wide range of source depths, from 0 km to 35 km, are searched in the inversion. We obtain a best-fitting source depth of 0.6 km, which provides a good fit to the observed *P*

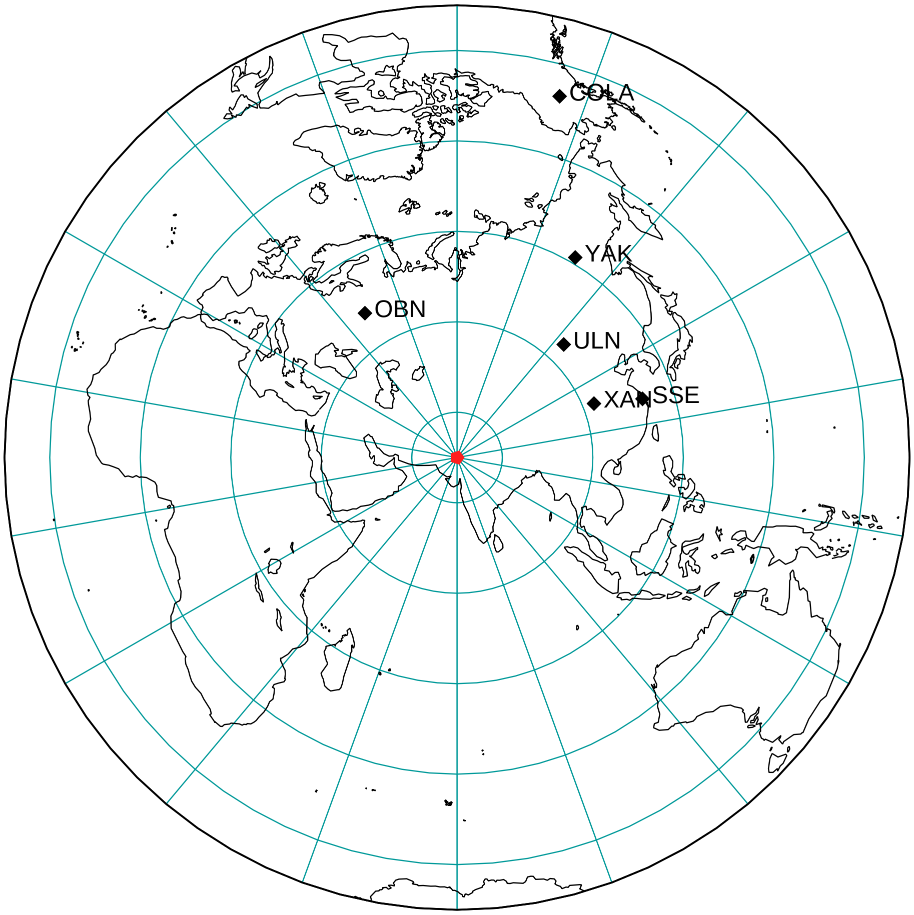

Fig. 5.20. Location of the 11 May 1998 Indian nuclear test along with the stations used in the inversion.

wave seismograms (Figure 5.21). Based on the depth estimate alone, we have grounds to suspect this event of being man-made. We use a moment tensor representation of the source mechanism, with no restriction on the allowable isotropic component. The source mechanism estimate we obtain is not wholly explosive, as it predicts the presence of a small amount of S wave radiation (Figure 5.21). We do, however, obtain a large isotropic component, and we estimate that the isotropic moment is at least 50% of the total moment, using the method of Bowers and Hudson (1999). This result is not really surprising, given the poor azimuthal coverage, and limited number of stations. The departure from an isotropic source mechanism is in the area where the P wave radiation pattern is not sampled due to lack of stations. If we had a few more stations, at different azimuths, we would be able to obtain better constraints on the source mechanism.

We cannot directly compare our depth estimate with the actual depth, as the Indian government has not released these details. However, we expect the depth of burial to

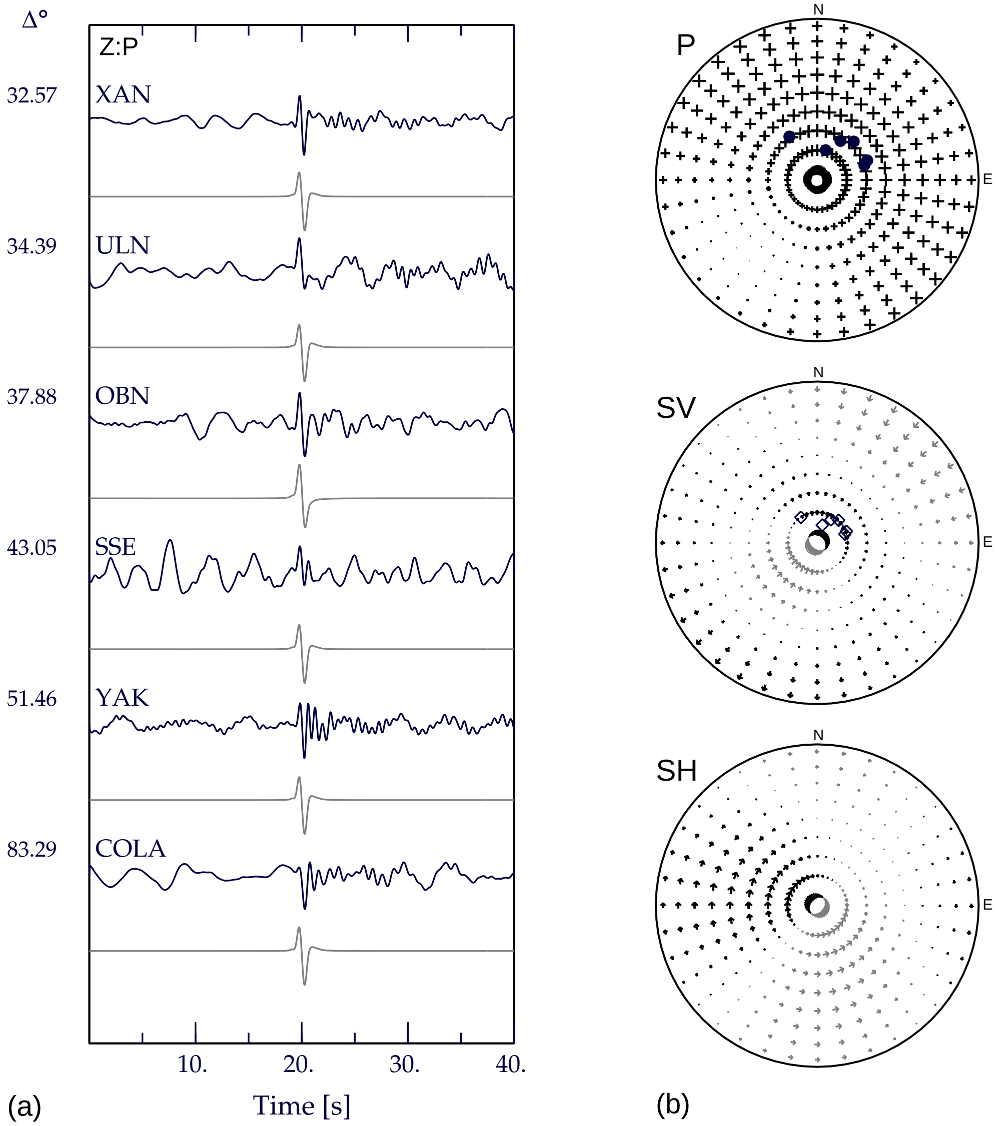

Fig. 5.21. Results of a *P* only waveform inversion for the 11 May 1998 Indian nuclear test. (a) Comparison between the observed (black traces) and predicted (grey traces) seismograms for the vertical component of *P*. The epicentral distances are displayed on the left, along with the station names. (b) Predicted *P*, *SV* and *SH* source radiation patterns obtained from the inversion.

be on the order of a few hundreds of metres. Given the very shallow depth estimate, and large isotropic component estimate, we have provided strong evidence to suspect this event of being a nuclear test. If this test had not been announced, our results with only a few stations would have provided grounds for further investigation.

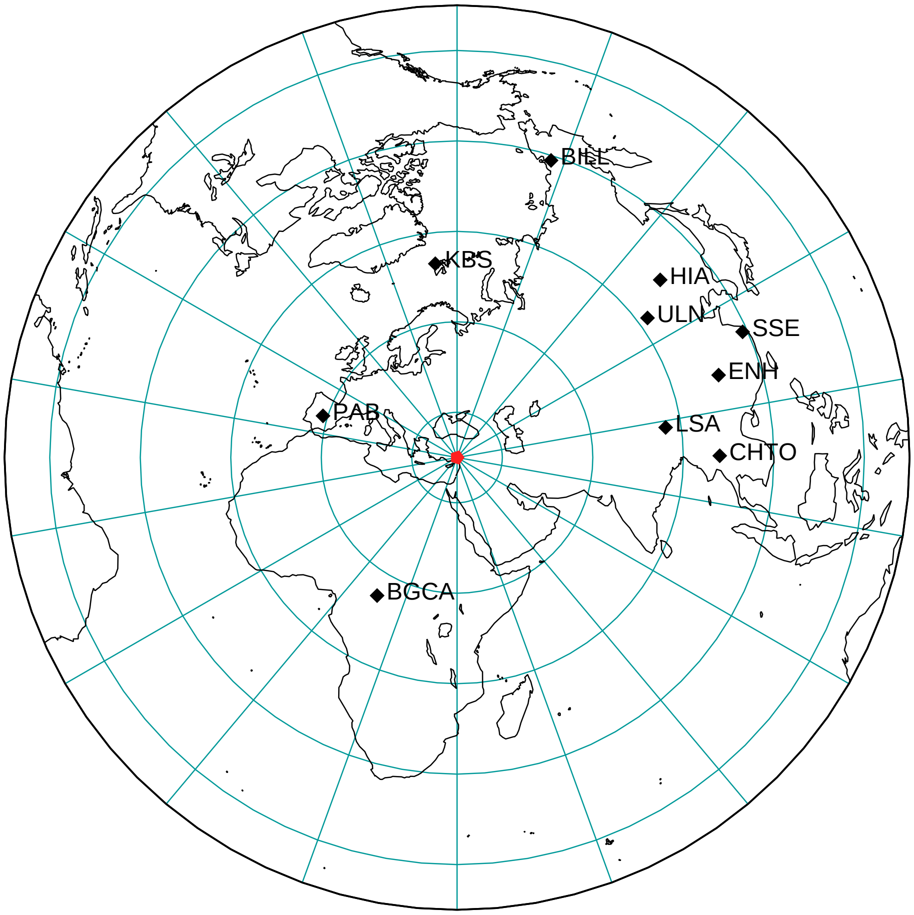

Fig. 5.22. Location of the 27 June 1998 Turkey event, along with the stations used in the inversion.

5.6 Turkey event

We perform inversion for an event which occurred in Turkey on 27 June 1998 (Figure 5.22). This event has an estimated m_b of 5.8, with a CMT depth estimate of 29.5 km. Thus we can again compare our inversion results with the CMT solution for this event (Dziewonski et al., 1999b). The waveforms used in the inversion have been obtained from the IRIS DMC. Ten stations are used in the inversion, but only five of the stations have suitable *SV* and *SH* waveforms due to low signal to *P* coda ratios for *S*. The waveforms are bandpass filtered in the range 0.01 Hz to 0.35 Hz before inversion.

We perform a joint *P* and *S* inversion, with a suitable weighting factor applied to the *S* wave data due to differing amounts of *P* and *S* information available. A moment tensor representation of the source mechanism is used, and we search over a wide range of source depths, from 0 km to 45 km. We obtain a depth estimate of 17 km, which fits the *P* wave seismograms reasonably well, but does not fit the *S* wave seismograms (Figure 5.23). We also obtain a poor fit to the CMT source mechanism (Figure 5.24),

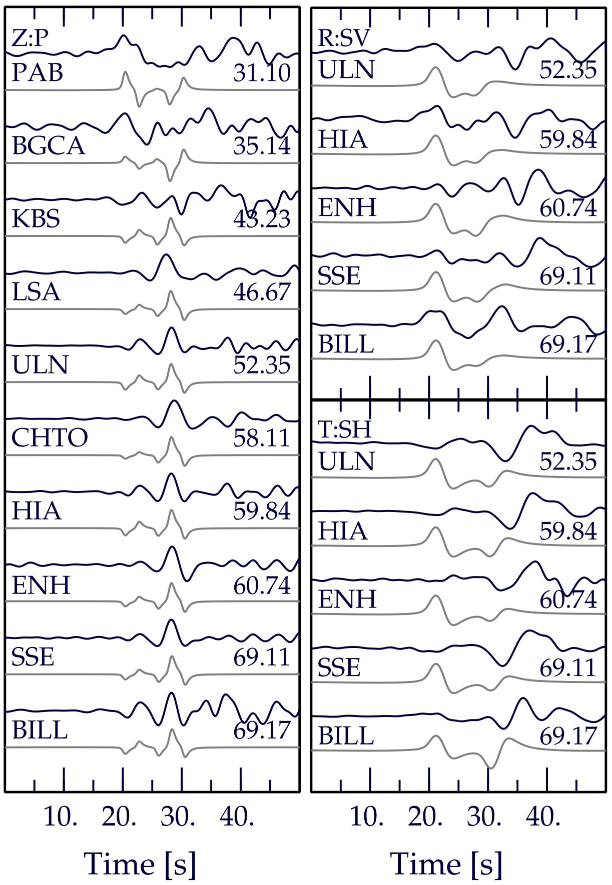

Fig. 5.23. Comparison between the observed (black traces) and predicted (grey traces) seismograms for the Turkey event. Shown are the vertical component of *P*, and the radial and transverse components of *S*. Each set of traces is annotated with the station name and epicentral distance.

although we do not obtain any significant isotropic component estimate. In this case the *P* information appears to be dominating the inversion, therefore we next perform an inversion using the *S* wave information alone. We obtain a depth estimate of 23 km, which provides a reasonable fit to the *S* wave seismograms, but again we obtain a poor fit to the CMT source mechanism. Thus we seem to get depth estimates which differ by 5 km, depending on whether we use *P* or *S* waveform information. In both cases the depth estimate is shallower than the CMT depth estimate.

Perhaps the difference in the depth estimates obtained from the inversion is due to variations in *P* and *S* velocities away from the *ak135* velocity model. We performed various experiments, adjusting the *P* and *S* velocities in the source crust, however changing the velocities by as much as 10% did not make a considerable difference to the result.

There seems to be evidence for variations in attenuation away from the reference

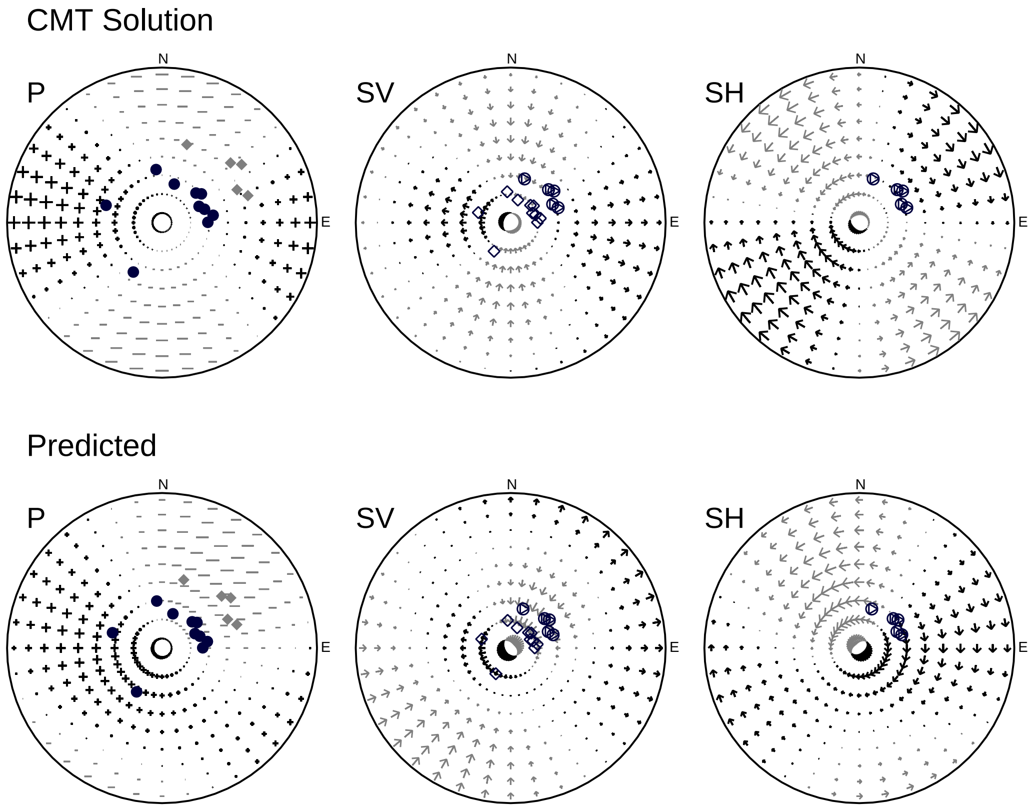

Fig. 5.24. Source radiation patterns for *P*, *SV* and *SH* waves for the Turkey event, using the CMT solution (top), and the predicted source mechanism obtained from the inversion (bottom). The plotted symbols represent the average take-off angle and azimuth for various phases; solid circles for *P*, solid triangles for *pP*, solid (grey) diamonds for *pS*; open circles for *S*, open triangles for *sS*, and open diamonds for *sP*.

model, as the observed waveforms seem more highly attenuated than the predicted waveforms. This effect was investigated by lowering *Q* in the *ak135* model, however it did not make any noticeable difference to the results.

It seems that the poor results we have obtained from this event are mainly due to the poor station distribution relative to the predominantly strike-slip source mechanism. Since we are using stations at teleseismic distances, we are mainly sampling areas of the radiation pattern where the *P* wave amplitude is very small, thus making it hard to identify direct *P*. Similarly, the direct *SH* arrival has small amplitude at all the stations, making it hard to identify. Also, the predominantly strike-slip source mechanism produces a certain symmetry. Due to this symmetry, and the fact that we have fairly poor azimuthal coverage, we are sampling similar areas of the source radiation pattern. We just do not have enough information on the relative arrival times between *P* and its surface reflected phases to obtain good depth constraints.

In an attempt to overcome these problems we tried applying a triangle shaped filter to the *P* waveforms. This is to try and boost the amplitude of the direct *P* arrival relative to the surface reflected phases, thereby making it easier to identify and subsequently align the direct *P* arrival. Unfortunately it is still hard to identify *P*, and this procedure did not make any difference to the results.

Despite the poor constraints on the source mechanism, we still get a reasonable depth estimate, and can confidently state that the source is midcrustal, ruling out a very shallow depth and the possibility of the event being an explosion. In addition, we do not obtain any significant isotropic component, which is encouraging. In the case of a predominantly strike-slip source mechanism it may be impossible to obtain well-constrained source parameters with only a few teleseismic stations. It has been noted by others (e.g., Wallace and Helmberger, 1982) that strike-slip events do not usually produce usable teleseismic *P* waves as little energy is radiated downward, however they often produce good regional waveforms. Therefore it should be possible to obtain better constraints by including some regional data and using more stations at different azimuths in order to obtain better sampling of the source radiation pattern.

5.7 India-Bangladesh border event

We perform inversion for an event which occurred on the India-Bangladesh border on 8 May 1997 (Figure 5.25). This event has an estimated m_b of 5.6, with a CMT depth estimate of 35 km. Thus we can again compare our inversion results with the CMT solution for this event (Dziewonski et al., 1999a). The waveforms used in the inversion have been obtained from the IRIS DMC. Ten stations are used in the inversion, but only seven of the stations have suitable *SV* and *SH* waveforms due to low signal to *P* coda ratios for *S*. The waveforms are bandpass filtered in the range 0.01 Hz to 0.7 Hz before inversion.

We perform a joint *P* and *S* inversion, with a suitable weighting factor applied to the *S* wave data due to differing amounts of *P* and *S* information available. A moment tensor representation of the source mechanism is used, and we search over a wide range of source depths, from 10 km to 45 km. A poor fit between the observed and predicted seismograms is obtained for both *P* and *S* (Figure 5.26). We also obtain a poor fit to the CMT source mechanism (Figure 5.27). The depth estimate obtained from the NA inversion is 33 km, which is close to the CMT depth estimate of 35 km, however the poor seismogram fit indicates that the inversion is not working for this event. This is probably due in part to the predominantly strike-slip source mechanism, producing problems similar to those discussed in Section 5.6 for the Turkey event. The direct *P*

Fig. 5.25. Location of the 8 May 1997 India-Bangladesh border event, along with the stations used in the inversion.

arrival has small amplitude at many of the stations, and there is a certain symmetry to the source radiation pattern, therefore we have the same problem of lack of source information at teleseismic distances.

A number of tests were performed to see if a better inversion result could be achieved. We checked the source location estimate used in the inversion against the location estimates appearing in the ISC bulletin, to see if large errors in the source location exist. The various source location estimates are similar, ruling this out as a possible cause of the problem. There also seems to be evidence that the observed seismograms are more highly attenuated than the synthetic seismograms, so the inversion was performed again with lower Q values. This did not make any noticeable improvement.

The location of this event, on the India-Bangladesh border, suggests that it is likely that shallow sediments are present at the source end. This could have quite

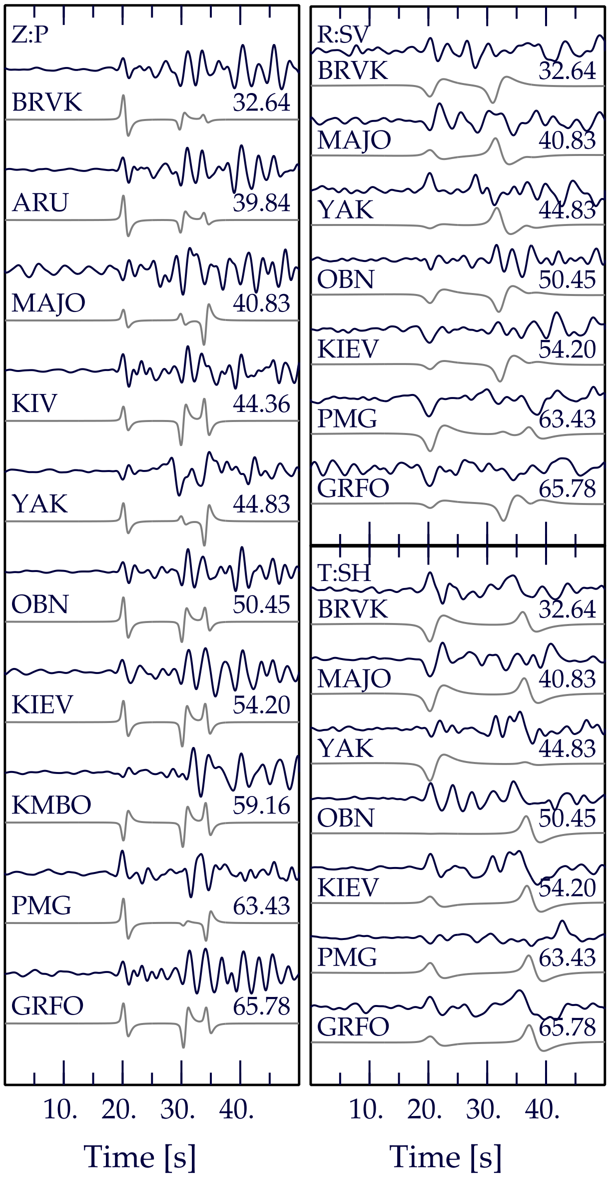

Fig. 5.26. Comparison between the observed (black traces) and predicted (grey traces) seismograms for the India-Bangladesh border event. Shown are the vertical component of *P*, and the radial and transverse components of *S*. Each set of traces is annotated with the station name and epicentral distance.

a pronounced effect on the seismograms, and could explain why the inversion is not working for this event. Initially, tests were performed with lowered surface velocities at the source end, but this did not improve the seismogram fit. The next step was to include a sediment layer at the source end, and calculate additional phases such as reflections off the bottom of the sediment, and first order reverberations in the sediment layer. A number of models for the sediment layer were tested, with thicknesses in the range 1-10 km, and *P* wave velocities of 5.4 km/s and 5.0 km/s with

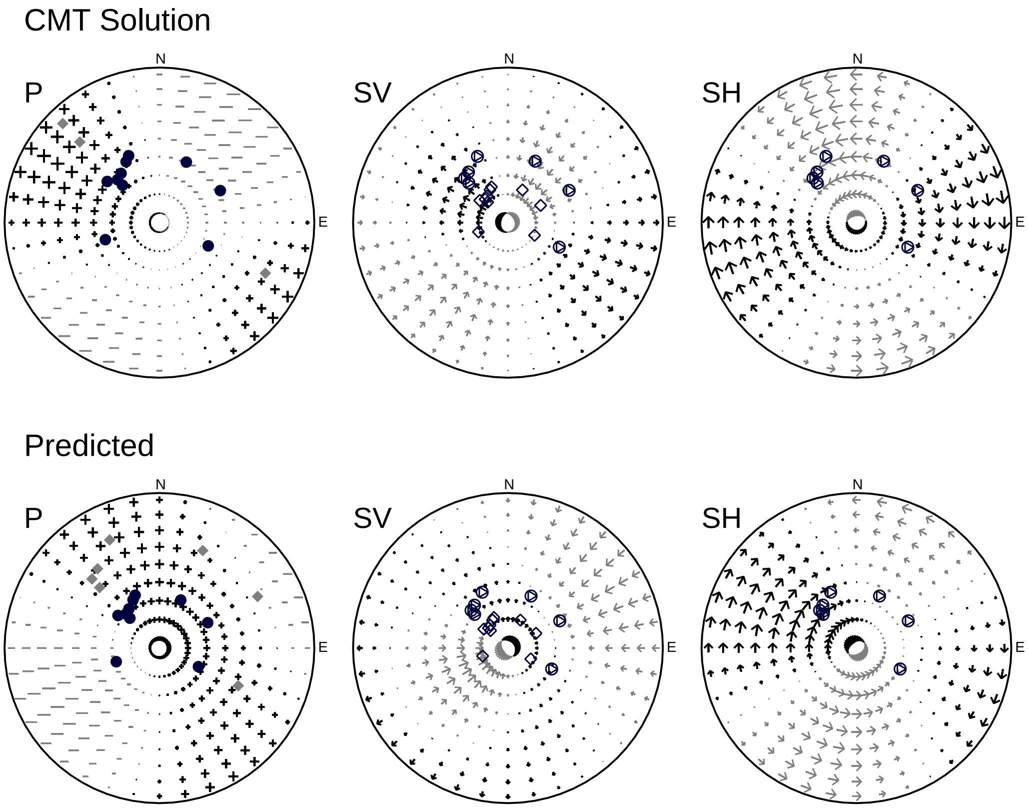

Fig. 5.27. Source radiation patterns for *P*, *SV* and *SH* waves for the India-Bangladesh border event, using the CMT solution (top), and the predicted source mechanism obtained from the inversion (bottom). The plotted symbols represent the average take-off angle and azimuth for various phases; solid circles for *P*, solid triangles for *pP*, solid (grey) diamonds for *pS*; open circles for *S*, open triangles for *sS*, and open diamonds for *sP*.

corresponding *S* wave velocities of 3.22 km/s and 2.98 km/s. Again, no significant improvement in the inversion was achieved.

The next test was to allow for a more complex source time function, as up until now we have been using a simple source time function consisting of a single trapezoid. We adapted the source time function to allow for two trapezoids shifted in time, and inverted for three extra model parameters; the time shift, the rise time of the second trapezoid, and the relative amplitudes of the two trapezoids. Even with the addition of a more complex source time function to the modelling, the fit between the observed and predicted seismograms was not improved.

It seems that the reason the inversion procedure does not work for this event is due to a breakdown of the assumptions used. The simple synthetic calculation scheme we are using is not sufficient to model the complex observed seismograms. The most likely explanation is the presence of lateral heterogeneity at the source

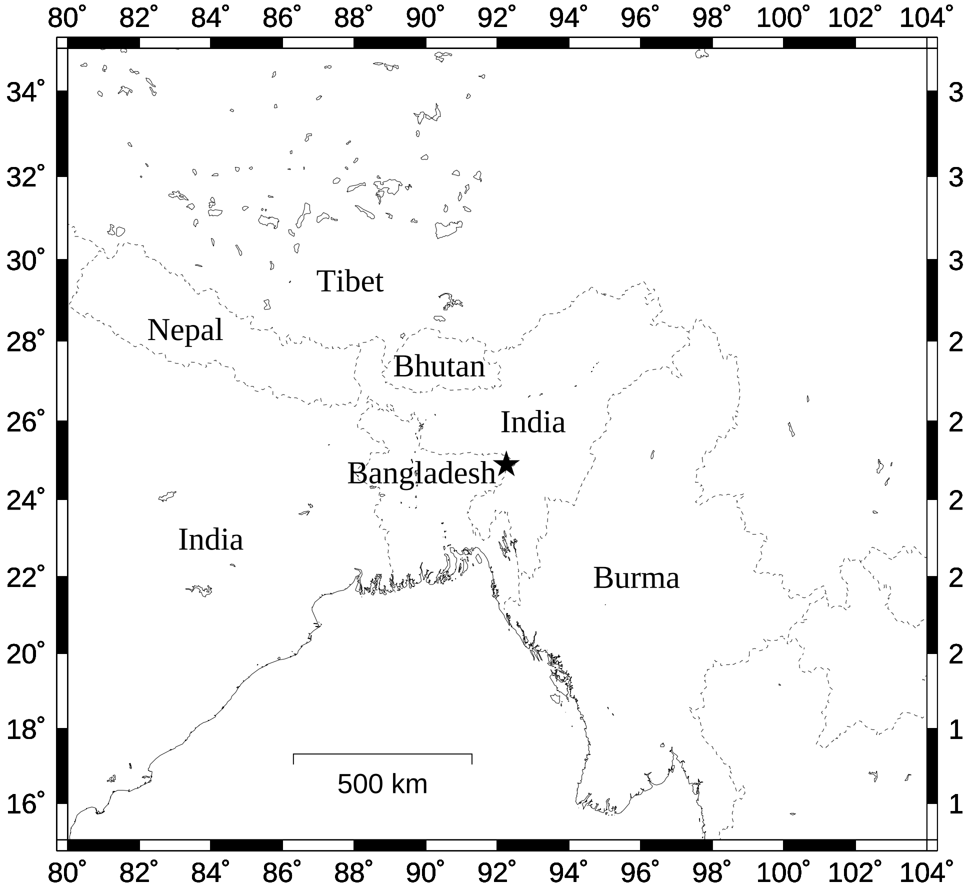

Fig. 5.28. Map of the source location of the India-Bangladesh border event (denoted by a star) and surrounding regions. The national borders are shown as dashed lines.

end. There is evidence for strong crustal heterogeneity in the vicinity of this event, with large topographic changes occurring close to the source location (see Figure 5.28). For example, the Himalayas lie approximately 250 km to the north of the event, and extending northwest. Waves leaving the source at different azimuths are therefore sampling different velocity structures. The four stations MAJO, YAK, KMBO and PMG exhibit observed *P* wave seismograms which are distinctly different to the seismograms recorded at the rest of the stations, which all lie approximately northwest of the event. Thus, it seems that the presence of strong crustal heterogeneity in the vicinity of this event has a pronounced effect on the observed seismograms, resulting in our inability to obtain a satisfactory seismogram fit using a simple modelling scheme. In order to model this event accurately, a region specific model allowing for lateral heterogeneity would need to be included at the source end.

5.8 Discussion

We have illustrated the performance of the NA source inversion with real data by studying six moderate sized events with a range of source depths. Even though we have used a rather simple synthetic seismogram calculation scheme, which has its limitations, we have demonstrated that good results are obtainable for moderate size events using relatively high quality data. For three of the events the source parameter estimates we obtain compare well with the CMT solution, which is encouraging. We were unable to obtain reliable results for two of the events, though this is not surprising given the station distribution relative to the predominantly strike-slip source mechanism for both events, and also the presence of strong crustal heterogeneity. The inversion also works well for nuclear explosions, as illustrated by its application to the 1998 Indian nuclear test.

Our investigations for the Honshu event reveal that it is necessary to allow for an improved representation of the structure above the source when performing inversion for sub-oceanic events. We can easily achieve this since we use a derivative-free inversion scheme with an allowance for different structures at the source and receiver ends. Even though we have used the *ak135* reference model throughout this study, there is little computational cost in using customised source and receiver models by modifying the near-surface velocities, thus changing the apparent amplification. Variations in *S* wave attenuation away from the reference model can be accommodated by modifying the mantle attenuation operator. A reasonably well constrained source depth was obtained for the Honshu event, even when the oceanic layer is not included, indicating that the depth estimate is relatively insensitive to the velocity model used. However, more accurate depth and mechanism estimates were obtained when a water layer above the source was incorporated into the model. This illustrates the need to identify whether events are suboceanic when an accurate depth and mechanism estimate is required, such as when monitoring the CTBT.

Inversion for both the southern Xinjiang and Kyrgyzstan events worked well using the standard *ak135* reference velocity model, as this provides a good representation of continental regions. A negligible explosive component was obtained for the Kyrgyzstan event, however, for the southern Xinjiang event quite a large implosive component was recovered due to the sampling distribution of the radiation pattern. It is possible that an introduced isotropic component may be compensating for deficiencies in the modelling, such as the use of a standard velocity model, resulting in an improved seismogram fit with the introduction of a small isotropic component.

Thus when testing the significance of any isotropic estimate, it may be best to allow for a small, but not significant isotropic component in the inversion.

The use of a derivative-free inversion method such as the NA has a number of advantages over linearised inversion; there is no dependence on the starting parameters, and various modelling complexities are easily included. The interface between the inversion and the waveform modelling is simple; the only information input into the forward modelling routine is the model parameters. In this way it is easy to substitute different modelling routines and even combine different schemes. We have demonstrated this flexibility for the event in southern Xinjiang by substituting more complex synthetic seismograms into the inversion scheme. In this case the use of ray theory is justified as similar results were obtained, however, the ability to use more accurate synthetics in the inversion may be useful for problematic events. In such cases the extra computational cost of calculating the synthetic seismograms would have to be weighed against the possible benefit.

Another advantage in using a derivative-free inversion scheme, based on only the rank of the misfit function, is that we can investigate the effects of using different misfit measures and are not restricted to the conventional squared residual measure. Tests with a number of different misfit measures for the southern Xinjiang event reveal that a L_3 norm measure, which is less tolerant to outliers, gives the best results.

One limitation of our source inversion method is that it does not directly provide any error bounds for the estimated model parameters, although the distribution of well fitting models in parameter space can provide a useful guide. It is possible to map the region of acceptable models found by the NA using the method of Farmer (2000). This gives an indication of the uncertainties associated with the best fitting model parameters. The application of this method to the southern Xinjiang event revealed a small, well defined region of acceptable models which indicates that the model parameters are well constrained, and that the best fitting model has small uncertainty associated with it. There also appears to be evidence for a trade-off between the length of the source time function and depth.

The discrimination capabilities of our method were illustrated by applying the inversion routine to the Indian nuclear test. This was treated in a similar way to the other events, with the inversion searching a wide range of source depths. A very shallow source depth was obtained, along with a large isotropic component estimate. If this test had not been announced, our results with only a few stations would have provided grounds for further investigation. This example also illustrates that our method works well using only P wave information.

We have been unable to obtain reliable inversion results for two of the events studied; the Turkey and India-Bangladesh border events. Both events appear to exhibit predominantly strike-slip faulting, and in such cases it may be impossible to obtain well-constrained source parameters with only a few teleseismic stations. Strike-slip events do not usually produce usable teleseismic *P* waves, but they often produce good regional waveforms, therefore it may be necessary to include regional data in the inversion for such events. In the case of the India-Bangladesh border event, its location in a region of strong crustal heterogeneity means that our simple modelling scheme is unable to obtain a reliable inversion result for this event. It is possible that the waveforms from the Turkey event are also affected by crustal heterogeneity, as the CMT source location estimate places the event near the East Anatolian fault. This is a fairly large left-lateral strike-slip fault, therefore significant lateral variations in the crust in this region are likely. We do, however, obtain depth estimates close to the CMT depth estimate for both events, which is encouraging and indicates that our method is able to obtain accurate depth estimates even for problematic events.